Origin of Activity in Cu-, Ru-, and Os-Mediated Radical Polymerization

Wade A Braunecker, William C Brown, Brian C Morelli, Wei Tang, Rinaldo Poli, Krzysztof Matyjaszewski

Origin of Activity in Cu-, Ru-, and Os-Mediated Radical Polymerization

Wade A. Braunecker,[a] William C. Brown,[a] Brian C. Morelli,[a] Wei Tang,[a] Rinaldo Poli,[b] and Krzysztof Matyjaszewski*[a]

[a]*Department of Chemistry, Carnegie Mellon University, 4400 Fifth Avenue, Pittsburgh, Pennsylvania 15213*

[b]*Laboratoire de Chimie de Coordination, 205 Route de Narbonne, 31077 Toulouse Cedex, France*

Email: km3b@andrew.cmu.edu

Abstract

A method is discussed for quantifying and categorizing the activity of an atom transfer radical polymerization (ATRP) catalyst as being derived from the product of its intrinsic reducing power and affinity for halide anions. The reducing power of several copper, ruthenium, and osmium ATRP catalysts was quantified with cyclic voltammetry in tetrahydrofuran, including for $MtX_2(PPh_3)_3$, $MtX(Cp^*)P^iPr_3$, and CuX(BPMODA) (where Mt = Ru and Os, X = Cl and Br, and BPMODA = N,N,-bis(2-pyridylmethyl)octadecylamine). Spectrophotometric measurements were used to determine ATRP equilibrium constants (K_{ATRP}), a measure of catalyst polymerization activity. Ru and Os catalysts of activity comparable to Cu are approximately 500 mV less reducing. Evaluation of kinetic polymerization data, together with $E_{1/2}$ and K_{ATRP} values, allowed the determination that halide affinities of these Ru and Os

compounds must be approximately 7-9 orders of magnitude stronger than typical Cu ATRP catalysts to compensate for their comparatively poor reducing power. Additionally, the ability of the coordinatively unsaturated Os compounds to control polystyrene molecular weights under organometallic radical polymerization (OMRP) conditions where the Ru analogues and Cu compounds cannot is discussed in terms of the potential for Os to form stronger Mt-C bonds. DFT calculations, ^{1}H NMR chain end analyses, and polymer chain extensions were conducted in order to evaluate the likelihood that standard halogen atom transfer (for ATRP) and reversible radical trapping (for OMRP) processes are indeed regulating the growing radical concentrations under the respective appropriate conditions with the new Os catalysts.

Keywords: Controlled radical polymerization, ATRP, OMRP, halide affinity, redox potential, osmium, ruthenium

Introduction

Since the initial discovery that complexes of Cu[1] and Ru[2] could mediate polymer molecular weights and molecular weight distributions in a technique known as atom transfer radical polymerization (ATRP), the development of more powerful and robust ATRP catalysts has fueled the synthesis of polymeric materials with an abundance of topologies, compositions, microstructures, and functionalities.[3-6] This technique employs a transition metal complex $Mt^{z}L_{n}$ to balance a population of dormant halide capped chains P-X and actively propagating radicals $P^{\bullet}$ through a redox process wherein the higher oxidation state metal halide complex $XMt^{z+1}L_{n}$ is reversibly generated (Scheme 1). The broader application of ATRP, as well as its mechanistic intricacies, has been thoroughly reviewed elsewhere.[7-9] Numerous structure-activity correlation

studies have provided guidelines for appropriately matching the activity and stability of an ATRP catalyst to a specific polymerization system, i.e., for controlling polymerization in protic media,[10,11] for polymerizing less reactive monomers,[12] for using low catalyst concentrations,[13-15] etc. However, successful ATRP remains elusive for a number of challenging systems which require exceptionally stable catalysts, as in acidic media or at low catalyst concentrations in aqueous media. A loss of control in these systems can partially be attributed to dissociation or hydrolysis of the metal-halide bond of the ATRP deactivator. The ability to screen catalysts based on their affinity for halide ions would thus be very beneficial.

Scheme 1. ATRP Mechanism.

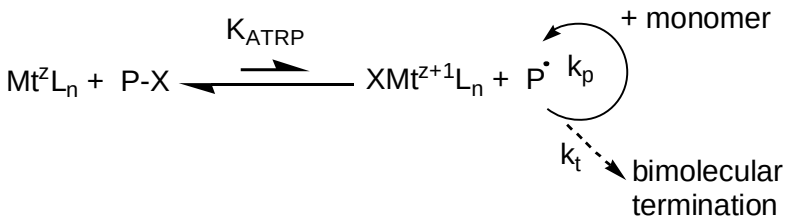

The rate of polymerization in ATRP, as defined in Eq. (1) (where k_p is the rate constant of propagation for a particular monomer, M), is ultimately governed by the position of the ATRP equilibrium. Quantifying K_{ATRP} for a given catalyst therefore provides an excellent measure of the catalyst's polymerization activity.[16]

$$R_p = k_p[M][P^\bullet] = k_p[M]K_{ATRP}\frac{[PX][Mt^zL_n]}{[XMt^{z+1}L_n]} \quad (1)$$

The ATRP equilibrium is defined by the relative homolytic bond strengths of the alkyl halide chain end and the Mt-X bond of the ATRP deactivator. K_{ATRP} can therefore in principle be expressed as the product of these two equilibria (Figure 1b, $K_{ATRP} = K_{BH}K_{Halo}$, where K_{BH} = P-X

bond homolysis and K_{Halo} = Mt-X bond homolysis, or "halogenophilicity" of the catalyst). This treatment of K_{ATRP} is experimentally verified in Figure 2, where a linear correlation is observed between values of K_{ATRP} measured for several alkyl halides with the same catalyst[16,17] (constant K_{Halo}) and values of K_{BH} calculated using DFT for the same alkyl halides.[18]

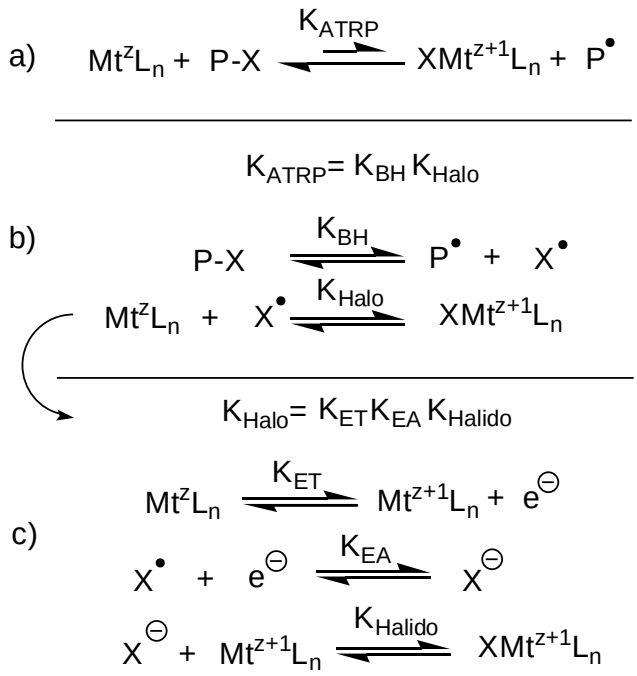

Figure 1. Representation of the ATRP equilibrium as a product of contributing reactions.

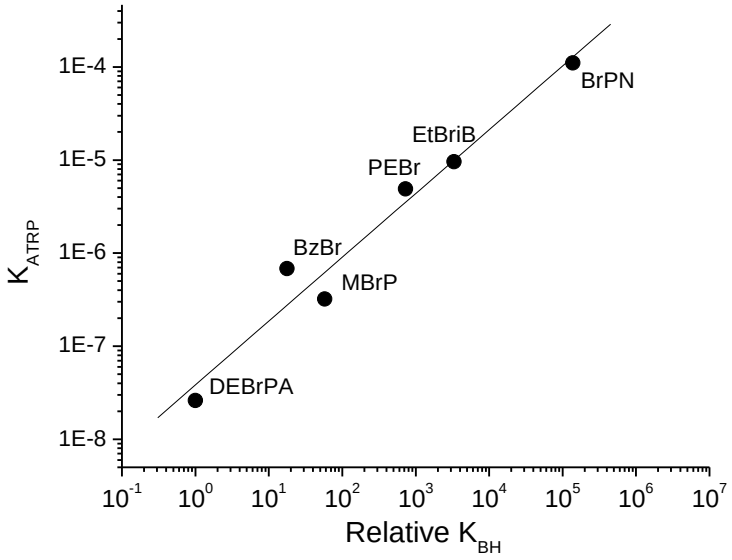

Figure 2. K_{ATRP} measured at 22 ºC with CuBr/tris(2-pyridylmethyl)amine;[16,17] relative values of K_{BH} determined from free energies calculated using DFT;[18] BrPN = bromopropionitrile, BzBr = benzyl bromide, DEBrPA = N,N-Diethyl-α-bromopropionamide, EtBriB = ethyl 2-bromoisobutyrate, PEBr = 1-(bromoethyl)benzene, MBrP = methyl 2-bromopropionate.

The halogenophilicity of a metal catalyst can also, in principle, be represented as the product of three reversible equilibria[19] (Figure 1c): i) oxidation of the metal complex (or equilibrium of electron transfer, K_{ET}); ii) reduction of a halogen to a halide ion (or electron affinity, K_{EA}); and iii) association of the halide ion to the higher oxidation state metal complex (or "halidophilicity", K_{Halido}). This treatment suggests that for a given alkyl halide (where K_{BH} and K_{EA} are constant), a linear correlation will exist between K_{ATRP} and the redox potential of a series of catalysts *when their affinity for halide anions is similar*, as defined in Eq. (2).

$$K_{ATRP} = K_{ET}K_{EA}K_{BH}K_{Halido} \quad (2)$$

Indeed, among structurally related complexes of the same metal, a linear correlation has generally been observed between the reducing power of a catalyst and its activity in ATRP for a series of Cu,[13,20-22] Fe,[23,24] and Ru-based catalysts.[25] The redox potentials of Ru compounds have also been correlated with their catalytic activity in the related process atom transfer radical addition (ATRA).[26] These experimental results further support the validity of Eq. (2). However, Cu and Ru catalysts of comparable activity have dramatically different redox potentials. Additionally, no correlation is observed between redox potentials and catalyst activity for a series of Ru catalysts with dramatically different structures.[27] These observations are a reflection of the relative halide affinity of the catalysts. We discuss herein how electrochemistry can be used as a tool, together with knowledge of an ATRP catalyst's activity, to indirectly measure

high values of halidophilicity. The method would be particularly useful for screening catalysts based on their affinity for halide ions as potential candidates for some of the aforementioned polymerization systems.

The application of Os compounds in synthetic polymer chemistry has been primarily limited to ring opening metathesis polymerization, where in some special cases Os catalysts either outperform[28] or show markedly different stereoselectivity[29] than their less expensive and more environmentally friendly Ru analogues. Only recently was it discovered that an Os complex could successfully mediate the controlled polymerization of styrene and (meth)acrylates under ATRP conditions.[30] While it has been known for some time that Os^{II} compounds are typically several hundred mV more reducing than their Ru analogues,[31] it seems this advantage Os complexes might have over Ru in terms of activity in ATRP has not yet been explored or appreciated. In addition, because of the vertical trend in transition metal-alkyl bond dissociation energies that tend to increase in a group in the order 3d < 4d < 5d,[32] Os^{II} may also be capable of mediating organometallic radical polymerization (OMRP, see Scheme 2) through the reversible formation of an Os^{III}-R bond.[30,33] Controlled radical polymerization by the OMRP mechanism was first reported for (porphyrin)Co^{II} complexes, giving dormant chains containing Co^{III}-(polymer) bonds.[34] An interplay between ATRP and OMRP was previously observed and well studied with Mo compounds[35-40] and also identified with Fe ATRP catalysts.[41] Therefore, the potential interplay of these mechanisms is also addressed in this work. The mechanism in which a metal species establishes control over a radical polymerization has dramatic implications on the absolute amount of complex ultimately required to successfully mediate the polymerization (*vide infra*). Thus, theoretical and experimental evidence are employed to conclusively demonstrate the role of these coordinatively unsaturated Os^{II} complexes in controlled radical polymerization.

Scheme 2. OMRP Mechanism.

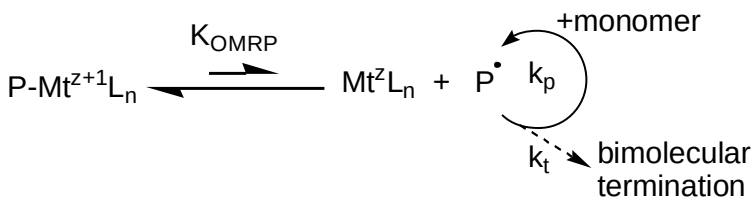

Experimental

Materials. $RuCl(Cp^*)P^iPr_3$,[42] $RuCl_2(Cp^*)P^iPr_3$,[43] $OsBr(Cp^*)P^iPr_3$,[44] $OsBr_2(Cp^*)P^iPr_3$,[44] $OsX_2(PPh_3)_3$,[45] $OsX_3(PPh_3)_3$,[46] and N,N,-bis(2-pyridylmethyl)octadecylamine) (BPMODA)[47] were synthesized according to literature procedures. All other complexes, reagents, and solvents used in this study were obtained from commercial sources. Tetrahydrofuran used in the determination of all equilibrium constants and in cyclic voltammetric measurements was distilled over CaH_2 under nitrogen prior to use. All monomers, ligands, and solvents were deoxygenated by purging with nitrogen for at least one hour prior to usage. Monomers were passed through a column of aluminum oxide to remove the radical inhibitor. 2,2'-Azobisisobutyronitrile (AIBN) and 2,2'- azobis(2,4-dimethyl-4-methoxy valeronitrile) (V-70) were recrystalized from cold methanol. Other reagents were used as received without further purification, unless otherwise noted.

Cyclic voltammetry. All voltammograms were recorded at room temperature with a PGSTAT100 instrument, using GPES (General Purpose Electrochemical System) version 4.9 AutoLab software. 1.0 mM solutions of the metal complex were prepared in dry, distilled THF containing 0.1 M Bu_4NPF_6 as the supporting electrolyte. Measurements were carried out under nitrogen at a scanning rate of 0.2 V s^{-1} using a glassy carbon disk as the working electrode, a platinum wire as the counter electrode, and a saturated calomel reference electrode.

General procedure for the determination of ATRP equilibrium constants (K_{ATRP}). The extinction coefficients of all Mt^zL_n and $XMt^{z+1}L_n$ complexes were first measured in THF by preparing solutions under nitrogen in a Schlenk flask joined to a quartz UV cuvette. Preformed Os and Ru complexes were allowed to stir for 20 minutes prior to any measurements, while Cu complexes formed in situ from CuCl or CuBr with 1.0 eq. of BPMODA stirred for 4 hours to ensure complete dissolution and formation. For determination of K_{ATRP}, ~1.0 mM solutions of the Mt^zL_n activator were prepared under nitrogen. The flask was transferred to a UV/Vis spectrometer. The appropriate initiator was transferred to the Schlenk flask via a nitrogen-purged micro-syringe. $XMt^{z+1}L_n$ concentration was calculated knowing the total concentration of metal species in solution and the extinction coefficients of the Mt^zL_n and $XMt^{z+1}L_n$ species at a given wavelength. The absorbance of the solution was monitored with time at a wavelength chosen to maximize the difference between the Mt^zL_n and $XMt^{z+1}L_n$ species (578 nm for RuCl(Cp*)P^{i}Pr$_3$ (Ru^{II} ε_{578} = 1250 , Ru^{III} ε_{578} = 180), 385 nm for OsBr(Cp*)P^{i}Pr$_3$ (Os^{II} ε_{385} = 750 $M^{-1}cm^{-1}$, Os^{III} ε_{385} = 1570 $M^{-1}cm^{-1}$), 820 nm for CuBr(BPMODA) (Cu^{II} ε_{820} = 400 $M^{-1}cm^{-1}$), and 790 nm for CuCl(BPMODA) (Cu^{II} ε_{790} = 200 $M^{-1}cm^{-1}$)). In this way, the concentration of deactivator generated in the system due to the persistent radical effect was followed with time. Two measurements were performed with each complex and the average value of K_{ATRP} is reported.

Polymerizations. A typical procedure follows. 2.0 mL of monomer and 0.2 mL of a diphenyl ether (DPE) internal standard were added to a nitrogen filled Schlenk flask containing a predetermined amount of the appropriate solid reagents (metal catalyst, ligand, AIBN). Deoxygenated solvent was then added when specified. After a 0.1 mL initial sample was taken at R.T. by nitrogen purged syringe, the solution was warmed to the desired reaction temperature in a thermostated oil bath. For ATRP reactions, the alkyl halide initiator was then injected into the

solution. Conversion and molecular weights were determined from periodic aliquots taken from the solution by gas chromatography (GC) and gel permeation chromatography (GPC), respectively.

ATRP Chain Extensions. A typical procedure follows. A polystyrene macroinitiator (PSty-Cl) was prepared under ATRP conditions with an Os catalyst ([Sty]:[PECl]:[$OsCl_2(PPh_3)_3$] = 200 : 1 : 1, 100 °C, bulk). The reaction was stopped after 30 minutes and quenched with dry acetone. PSty-Cl was isolated by precipitation in dry methanol, then redissolved in dry toluene and heated at 100 °C for one hour while open to the atmosphere. The solution was then cooled, and PSty-Cl was precipitated/washed with methanol and redissolved in acetone 6x to remove any residual metal species. PSty-Cl (M_n = 4200 g/mol) was dried overnight in a vacuum oven, and then chain extended to 42,000 g/mol with a CuCl catalyst ([Sty]:[PSty-Cl]:[CuCl]:[$CuCl_2$]:[BPMODA] = 200 : 1 : 1 : 0.1 : 1.1, 100 °C, bulk, ~20 h) .

Analyses. Monomer conversion was determined by GC using a Shimadzu GC 14-A gas chromatograph equipped with a FID detector and J&W Scientific 30 m DB WAX Megabore column. The initial temperature was 40 °C (3 minute hold) and final temperature 180 °C (6 minute hold) with a heating rate of 40 °C/min. Before determination of molecular weights, the samples were diluted with THF and then filtered through a short column of neutral alumina followed by a 0.2 μm PTFE Acrodisc filter. Molecular weight distributions were determined on a GPC system consisting of a Waters 515 pump, a Waters 717plus autoinjector, Polymer Standards Service columns (styrogel 10^5, 10^3, 10^2 Å), and a Waters 2410 RI detector against polystyrene standards using THF as the eluent at a flow rate of 1 mL/min at room temperature. Diphenyl ether was employed as an internal standard. All ^{1}H NMR spectra were obtained using a

Bruker Avance AV-300 (operating at 300.13 MHz). All spectroscopic measurements were performed on a Cary 5000 UV/VIS/NIR spectrometer (Varian).

Kinetic Modeling. The Predici program (version 6.3.1) was used for all kinetic modeling and employs an adaptive Rothe method as a numerical strategy for time discretization.[48] The concentrations of all species can be followed with time.

Computational Details. All calculations were performed using the B3LYP three-parameter hybrid density functional method of Becke,[49] as implemented in the Gaussian03 suite of programs.[50] All geometry optimizations were performed with no symmetry restrictions and all optimized geometries were characterized as local minima of the potential energy surface (PES) by verifying that all second derivatives of the energy were positive. The spin unrestricted formulation was used for the doublet states; the spin contamination was found to be negligible in all cases. The maximum deviation of the mean value of the S^2 operator from the theoretical value of 0.75 was 0.782 for the carbon-based styryl radical, $PhCHCH_3$. The chlorine atom and all metal complexes gave values much closer to the theory (0.752 - 0.776). The basis sets used for the geometry optimizations are the standard 6-31G* for C, H and P and Cl atoms, and the standard LANL2DZ basis set, which included the Hay and Wadt effective core potentials (ECP),[51] for the osmium and ruthenium atoms. To the basis set of the metal atoms, however, was added a single *f*-type polarization function ($\alpha = 0.8$) in order to obtain a balanced basis set and to improve the angular flexibility of the metal functions. All energies were corrected for zero point vibrational energy and for thermal energy to obtain the bond dissociation enthalpies at 298 K. An entropy correction was applied to obtain the Gibbs Free Energy at 298 K. The standard approximations for estimating the thermochemical corrections were used (ideal gas, rigid rotor and harmonic oscillator) as implemented into Gaussian03.

Results and Discussion

A. Electrochemical Measurements.

The complexes investigated in this study were specifically chosen to cover a broad range in activity. $RuCl_2(PPh_3)_3$ and analogues of $RuCl(Cp^*)P^iPr_3$ represent some of the least and most active Ru catalysts employed to date in ATRP.[25] Os^{II}-based complexes are typically much more reducing than their Ru analogues (by several hundred mV), as a result of the inherent stability of 3rd row metals in a higher oxidation state vs. those in the 2nd row,[31,52,53] and therefore warrant investigation as potential ATRP catalysts. All of the Ru and Os compounds employed in the model studies are coordinatively unsaturated 16 electron species that are well characterized in the literature. The ATRP deactivator can be formed from these complexes as illustrated in Scheme 1 through direct halogen atom abstraction from an alkyl halide without first requiring the dissociation of a phosphine ligand or the slipping of the Cp* ring. Such prerequisites for coordinatively saturated ATRP activators might complicate the measuring of any equilibrium constants or the interpretation of the data.

Acetonitrile has typically been employed in cyclic voltammetric studies of Fe and Cu ATRP catalysts with polydentate ligands to ensure sufficient solubility of the metal species. Chlorinated solvents have been used in the study of Ru with monodentate ligands. However, in order to avoid halogen abstraction from the solvent by the more active catalysts, and displacement of weakly bound monodentate ligands by acetonitrile, THF was employed as the medium in this work. The use of THF does, however, limit the number of sufficiently soluble Cu compounds that can be studied in the relatively non-polar medium. A summary of all cyclic voltammetric

data is recorded in Table 1, where the compounds investigated are arranged in order of their measured reducing power.

Table 1. Electrochemical data for $Cu^{I/II}$, $Ru^{II/III}$, and $Os^{II/III}$ couples measured in THF at 22 °C.[a]

Complex	**$E_{1/2}$, V**
$RuCl_2(PPh_3)_3$	0.67
Ferrocene	0.55
$OsCl_2(PPh_3)_3$	0.50
$OsBr_2(PPh_3)_3$	0.43
$RuCl(Cp^*)P^iPr_3$	0.42
$OsBr(Cp^*)P^iPr_3$	0.20
CuBr(BPMODA)	-0.04
CuCl(BPMODA)	-0.14

[a)] Quasi-reversible; 0.1 M NBu_4PF_6, 1 mM metal complex, scan rate 0.2 V s^{-1}; potentials reported vs. SCE.

The trends observed in THF in this work parallel those previously reported in other organic solvents. For example, CuCl(BPMODA) is 100 mV more reducing than the bromide analogue in THF, similar to acetonitrile wherein CuCl with the analogous N,N,-bis(2-pyridylmethyl)octylamine) (BPMOA) is 140 mV more reducing than CuBr(BPMOA) (-0.04 V and -0.18 V vs. SCE in acetonitrile).[20] $RuCl(Cp^*)P^iPr_3$ is 250 mV more reducing than $RuCl_2(PPh_3)_3$ in THF. The structurally related but coordinatively saturated $RuCl(Cp^*)(PPh_3)_2$ is 310 mV more reducing than $RuCl_2(PPh_3)_3$ in dichloroethane (0.46 V and. 0.77 V vs. Ag/AgCl in dichloroethane).[25]

The $E_{1/2}$ values in Table 1 are also consistent with other trends found in the literature, i.e., that Os compounds are several hundred mV more reducing than their Ru analogues, and that

complexes with the electron donating Cp* ligand are several hundred mV more reducing than the metal halide species bound only with monodentate phosphine ligands. As a difference in 59 mV in the reducing power of two complexes corresponds at 298 ºK to one order of magnitude in K_{ET} (according to the Nernst equation), electrochemistry therefore suggests these Os compounds would be 3-4 orders of magnitude more active in ATRP than their Ru analogues, and that the $MtX(Cp^*)P^iPr_3$ catalysts would also be about 4 orders of magnitude more active than $MtX_2(PPh_3)_3$ (assuming all other factors equal, i.e., the halidophilicity of the different compounds).

B. Quantification of K_{ATRP}

ATRP catalyst activity is often evaluated by the rate at which the catalyst mediates polymerization, which is entirely accurate under appropriate conditions. However, exceptionally active catalysts can generate a large amount of radicals that terminate by coupling before equilibrium in a system is reached, causing the higher oxidation state metal deactivator to accumulate at the beginning of the reaction and slow the polymerization according to Eq. (3). Consequently, if the appropriate amount of persistent radical deactivator is not present prior to the introduction of the alkyl halide initiator, it is often observed that highly active catalysts actually mediate slower polymerizations in ATRP.[13] Quantification of K_{ATRP} via model reactions therefore provides an excellent measure of the true activity of an ATRP catalyst.

This can be accomplished through spectroscopic monitoring of the time dependent deactivator accumulation according to the persistent radical effect, for which precise equations were recently derived and the wide applicability of the approach was demonstrated.[16] For 1:1 stoichiometry ($[Mt^zL_n]_0 = [RX]_0$), the values of a function $F([XMt^{z+1}L_n])$ defined in Eq. (3) are

plotted against time, and K_{ATRP} is obtained from the slope of the linear dependence. When an excess of alkyl halide initiator to activator is employed, the time dependence of deactivator accumulation is more complex (Eq. (1S)).

$$F\left(\left[XMt^{z+1}L_n\right]\right) \equiv \frac{\left[Mt^zL_n\right]_0^2}{3\left(\left[Mt^zL_n\right]_0 - \left[XMt^{z+1}L_n\right]\right)^3} - \frac{\left[Mt^zL_n\right]_0}{\left(\left[Mt^zL_n\right]_0 - \left[XMt^{z+1}L_n\right]\right)^2} + \frac{1}{\left[Mt^zL_n\right]_0 - \left[XMt^{z+1}L_n\right]} = \quad (3)$$
$$= 2k_tK_{ATRP}^2t + \frac{1}{3\left[Mt^zL_n\right]_0}$$

While it is later demonstrated that the Os^{II} ATRP catalysts employed in this investigation can also participate in organometallic radical polymerization (OMRP) trapping reactions to generate R-Os^{III} species, experimental evidence (*vide infra*) illustrates that the fraction [R-Os^{III}]/[Os_{Total}] generated during polymerization and during model experiments is very small (≤ 1 %). The assumption was therefore made that the OMRP reaction could be neglected in the determination of K_{ATRP} for the Os compounds with this method. PREDICI simulations, which have been employed for detailed kinetic analyses of controlled radical polymerizations,[54-56] are used in the supporting information to confirm the validity of these assumptions.

Having independently measured the extinction coefficients of the ATRP activator and deactivator in THF for all catalysts under investigation (see Figure 3 and Figures 1S – 3S), the absorbance of the solution was monitored with time at a wavelength chosen to maximize the difference between the Mt^zL_n and $XMt^{z+1}L_n$ species, and deactivator concentration calculated knowing the total concentration of metal species. Representative plots of deactivator accumulation with time and F([$XMt^{z+1}L_n$]) vs. time are illustrated in Figure 4 for the

determination of K_{ATRP} of RuCl(Cp*)P^{i}Pr$_3$ with 1-phenylethyl chloride (PECl). The results for all complexes investigated are summarized in Table 2 and illustrated in Figures 4S – 10S.

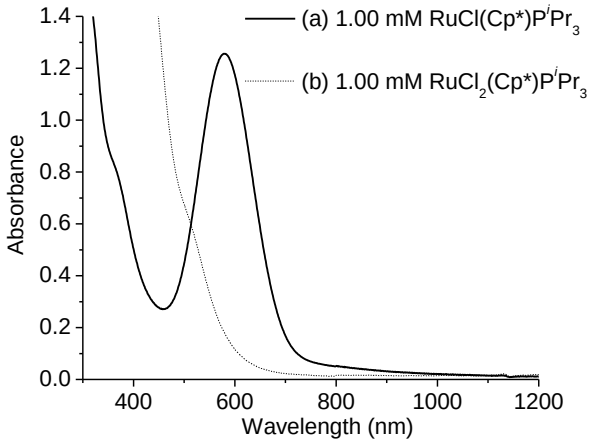

Figure 3. 1.00 mM electronic spectra of (a) RuCl(Cp*)P^{i}Pr$_3$ and (b) RuCl$_2$(Cp*)P^{i}Pr$_3$. Change in absorbance at 578 nm later followed for determination of K_{ATRP}.

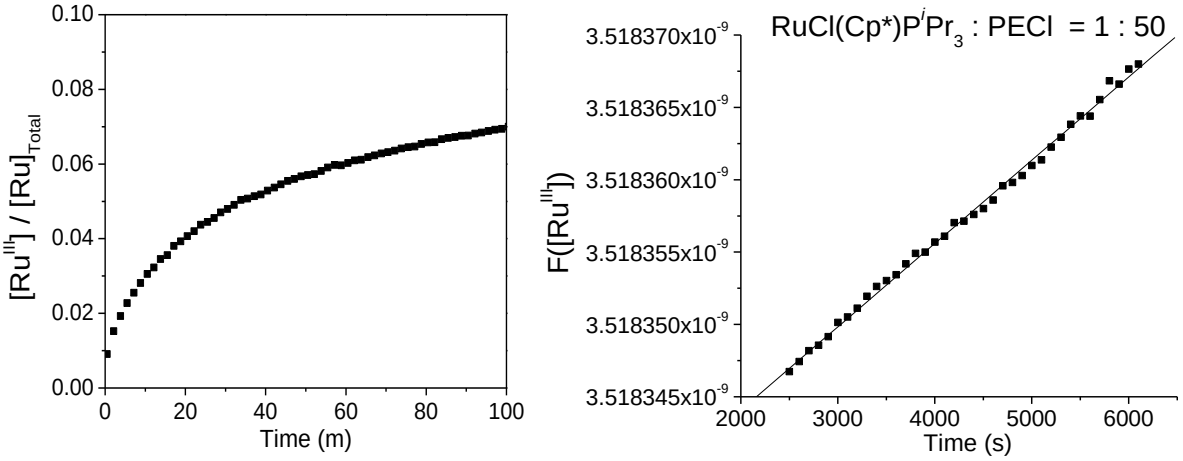

Figure 4. Determination of K_{ATRP} for the reaction of RuCl(Cp*)P^{i}Pr$_3$ (0.89 mM) with 50 eq. PECl in THF: a) accumulation of Ru^{III} deactivator with time and b) plot of F([RuCl$_2$(Cp*)P^{i}Pr$_3$]) against time.

Table 2. Summary of K_{ATRP} and redox data in THF at 22 °C.[a]

Complex	Initiator / Catalyst	K_{ATRP}	$E_{1/2}$

$OsBr_2(PPh_3)_3$	EtBrPhAc	100/1	3.1×10^{-6}	0.43
$RuCl(Cp^*)P^iPr_3$	EtClPhAc	1 / 1	2.1×10^{-4}	0.42
	PECl	50/1	2.0×10^{-9}	
$OsBr(Cp^*)P^iPr_3$	PEBr	1 / 1	3.2×10^{-5}	0.20
	BzBr	1 / 1	2.0×10^{-6}	
CuBr(BPMODA)	EtBrPhAc	1 / 1	1.1×10^{-4}	-0.04
	PEBr	10/1	4.0×10^{-9}	
CuCl(BPMODA)	PECl	50/1	4.8×10^{-10}	-0.14

[a)] EtClPhAc = ethyl α-chlorophenylacetate, EtBrPhAc = ethyl α-bromophenylacetate, PECl = 1-phenylethyl chloride, PEBr = 1-phenylethyl bromide, BzBr = benzyl bromide.

The K_{ATRP} value for CuX(BPMODA) with PEBr (X = Br) is one order of magnitude higher than with PECl (X = Cl), despite the fact that the CuCl complex is more reducing. This is consistent with literature results in acetonitrile[16] and fully consistent with the breakdown of the ATRP equilibrium in Figure 1, as the homolytic C-Cl bond strength is significantly greater than that of C-Br.[18] The K_{ATRP} value of 4.0×10^{-9} measured for CuBr(BPMODA) with PEBr in THF is also in relatively good agreement with a value of 3.0×10^{-8} determined for CuBr in acetonitrile with analogous N,N,-bis(2-pyridylmethyl)propylamine) (BPMPrA) scaled against PEBr.[13]

As a new ATRP catalyst, it is important to verify that $OsBr(Cp^*)P^iPr_3$ mediates radical polymerization according to the ATRP mechanism, especially given the propensity of these complexes to form stronger Mt-C bonds that Ru. This is indeed verified in a later section. The value of K_{ATRP} determined for $OsBr(Cp^*)P^iPr_3$ with PEBr is about 20 times faster than BzBr, also consistent with literature values for these two initiators with Cu-based catalysts in acetonitrile.[16] $OsBr(Cp^*)P^iPr_3$ was measured as over 10,000 times more active than its ruthenium chloride analogue with PECl. With a K_{ATRP} value of 3.2×10^{-5}, this ranks the Os complex as one

of the most active ATRP catalysts known to date (compare with CuBr/Me_6TREN in Figure 5, K_{ATRP} scaled against PEBr in acetonitrile is 7.3×10^{-5}).[16]

The high relative activity of OsBrCp*P^{i}Pr$_3$ with PEBr can be rationalized as a function of several contributing factors: CuBr compounds are often 100 mV less reducing than CuCl, yet, as a function of several offsetting factors (including weaker R-Br bond dissociation energy, but lower electron affinity of Br and lower bromidophilicity of Cu), a 10-fold increase in ATRP activity is typically observed on going from CuCl/R-Cl to CuBr/R-Br. In contrast, the redox potentials of OsBr compounds in the literature are often more similar to OsCl compounds. $OsBr_2(PPh_3)_3$ was even measured as slightly more reducing than $OsCl_2(PPh_3)_3$ in this study. One should therefore expect to see a significantly larger increase in ATRP activity upon going from OsCl compounds to OsBr than is observed when going from CuCl to CuBr. Additionally, the ratio of Os^{III} bromidophilicity / chloridophilicity is expected to be greater than that for Ru or Cu, based on hard-soft acid-base theory, resulting in a further relative increase in activity on going from OsCl to OsBr as compared with Ru or Cu.

Under the conditions employed, a reaction of RuCl(Cp*)P^{i}Pr$_3$ with 50 eq. of PECl proceeded to less than 10% conversion in 100 min. (Figure 4). As the activity of this catalyst is at the lower limit of what is measureable with PECl, a significantly more active initiator would be necessary to measure K_{ATRP} of the less active $MtX_2(PPh_3)_3$ compounds. Ethyl α-chlorophenylacetate (EtClPhAc) proved 5 orders of magnitude more active than PECl with RuCl(Cp*)P^{i}Pr$_3$, as did ethyl α-bromophenylacetate (EtBrPhAc) over PEBr with CuBr(BPMODA), making these initiators ideally suited for K_{ATRP} determination of less active catalysts. $RuCl_2(PPh_3)_3$ is known to partially dissociate a PPh_3 ligand and subsequently dimerize in solution,[45] making the accurate determination of K_{ATRP} of the compound impossible with this technique. However, the Os

analogues are reportedly stable,[45] allowing K_{ATRP} of $OsBr_2(PPh_3)_3$ to be measured with EtBrPhAc.

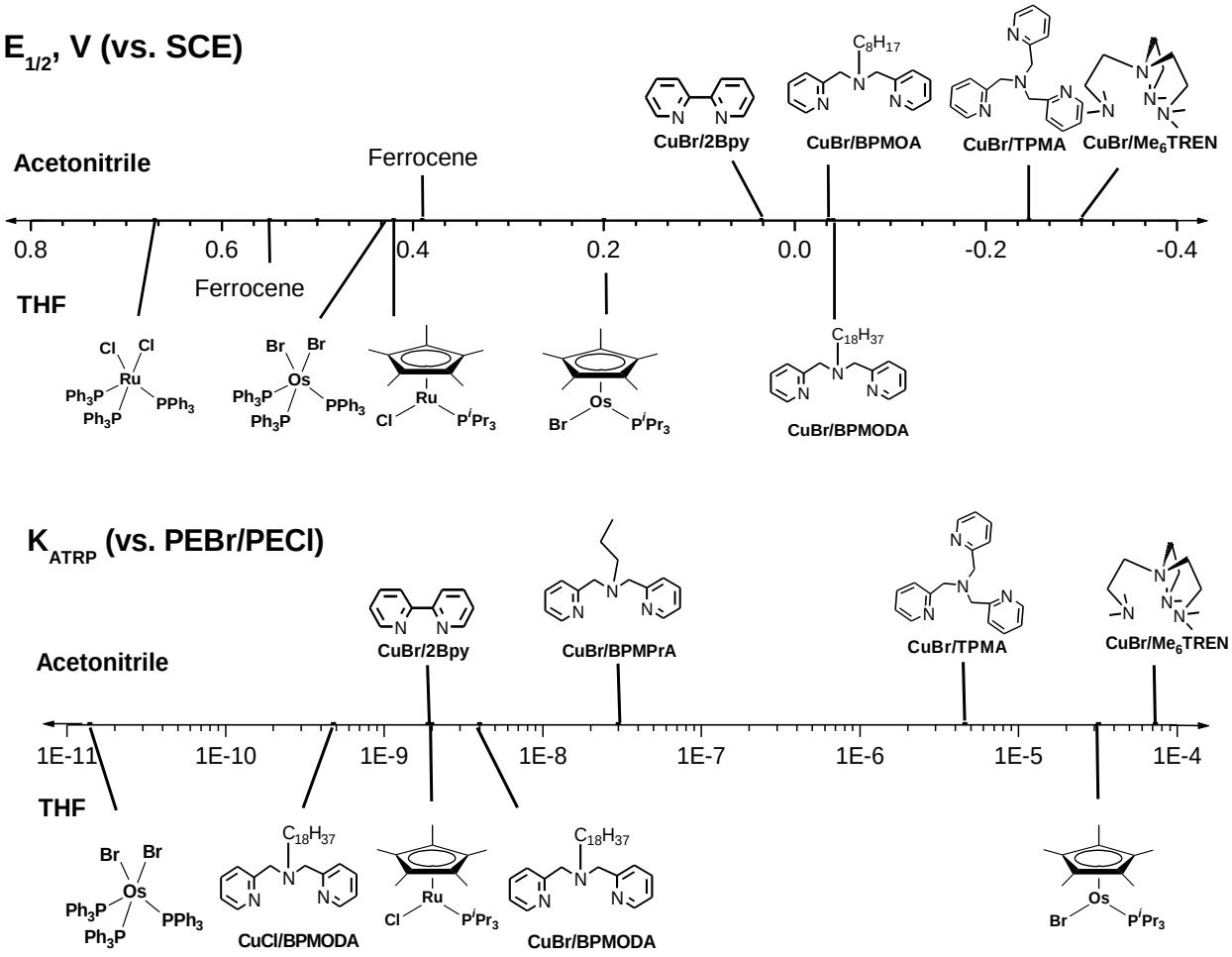

Figure 5. A comparison of $E_{1/2}$ [20] and K_{ATRP} [16] values for Cu compounds measured in acetonitrile with values of Cu, Ru, and Os compounds measured in THF.

A summary of data collected in THF and relevant literature data collected in acetonitrile is illustrated in Figure 5. Further analysis of the data reveals that despite $OsBr(Cp^*)P^iPr_3$ being 240 mV less reducing than CuBr(BPMODA) (a value of K_{ET} four orders of magnitude lower), it has

an 8000 times higher value of K_{ATRP}. With K_{BH} and K_{EA} in these two systems remaining constant, Eq. (1) suggests the halidophilicity of this Os complex must be 7-8 orders of magnitude greater than Cu to compensate for its comparatively poor reducing power. Similarly, RuCl(Cp*)P^{i}Pr$_3$ is 560 mV less reducing than CuCl(BPMODA), yet 3 times more active in ATRP. Eq. (1) suggests the halidophilicity of this Ru complex is more than 9 orders of magnitude greater than that of Cu. Little data is available on the halidophilicity of Ru^{III} compounds in organic solvents in the literature, as the high equilibrium constants are difficult to measure using spectroscopic techniques. It was reported for some Ru^{III}-cyclam complexes that chloride dissociation in aqueous media could not be detected using spectrophotometric techniques, even at elevated temperatures over the course of several days.[57] Chloridophilicity was estimated in this system as greater than 10^6 M^{-1} (whereas typical Cu^{II} ATRP catalysts have values of halidophilicity on the order of 10 M^{-1} in water rich solvents[10]).

C. Atom Transfer Radical Polymerization

In an effort to support the validity of K_{ATRP} values quantified with model experiments in the preceding section, rates of polymerization mediated by these catalysts are now compared. It is not possible to evaluate all catalysts in this study under the same polymerization conditions given that differences in their activity span many orders of magnitude. However, K_{ATRP} measured for RuCl(Cp*)P^{i}Pr$_3$ and CuCl(BPMODA) at room temperature differed by less than a factor of three. These catalysts should therefore mediate ATRP at a similar rate.

Three polymerizations were conducted, one each catalyzed by CuCl(BPMODA), RuCl(Cp*)P^{i}Pr$_3$, and RuCl(Cp*)(P^{i}Pr$_3$)$_2$ (the latter being generated in situ with the addition of one extra equivalent of P^{i}Pr$_3$). In all cases, 10% of the appropriate deactivator was added from

the beginning of the reaction to minimize radical termination reactions that might disproportionately affect the rate of one polymerization over another. Room temperature polymerization was extremely slow; even at 60 °C, approximately 170 h were needed to reach 80% conversion. The results are illustrated in Figure 6.

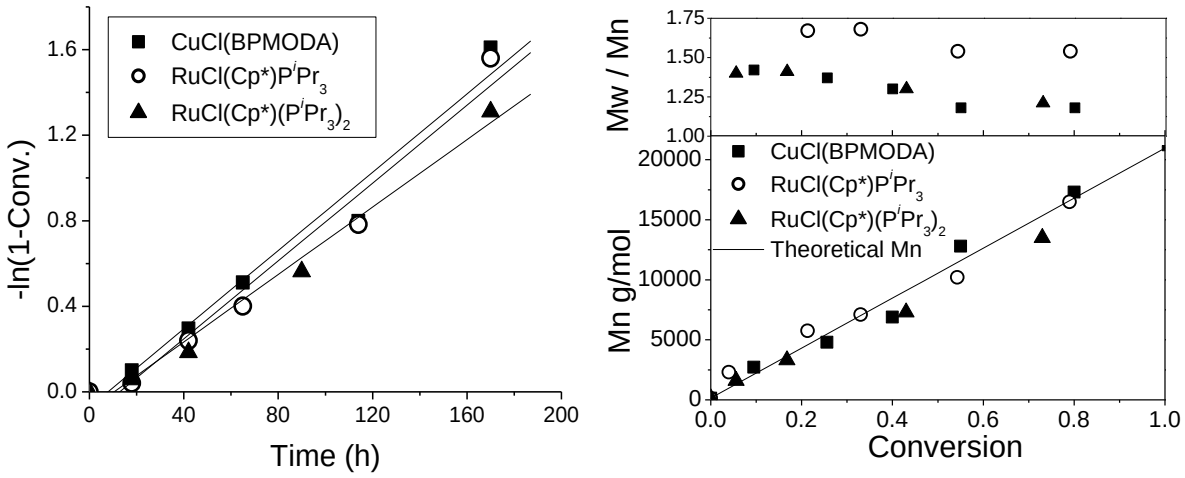

Figure 6. ATRP of bulk styrene at 60 °C ([Sty]: [PECl] : [Mt^{z}L] : [XMt^{z+1}L] = 200 : 1 : 1 : 0.1) mediated by CuCl(BPMODA), RuCl(Cp*)P^{i}Pr$_3$, and RuCl(Cp*)(P^{i}Pr$_3$)$_2$; 10% diphenyl ether internal standard.

The rates of polymerization catalyzed by CuCl(BPMODA) and RuCl(Cp*)P^{i}Pr$_3$ were nearly identical, as predicted from their similar values of K_{ATRP}. However, while control over polystyrene molecular weight distribution at high conversion with Cu and with the 18 electron Ru species was good (M_w/M_n ~ 1.2), the 16 electron Ru species exhibited worse control (M_w/M_n > 1.5). This observation is consistent with literature reports that an 18 electron RuCl(Cp*)(PPh$_3$)$_2$ complex can adequately control styrene under ATRP conditions, while the 16 electron complex RuCl(Cp*)PCy$_3$ demonstrated much worse control.[58] Regardless, the kinetic polymerization data confirms that the ATRP equilibrium constants are similar for the Ru and Cu catalysts.

Under the same conditions ([Sty]: [PEBr] : [Mt^zL] : [$XMt^{z+1}L$] = 200 : 1 : 1 : 0.1, bulk, 60 °C), initiation efficiency in the ATRP of styrene catalyzed by $OsBr(Cp^*)P^iPr_3$ was low (~60 %, see Figure 11S). When the polymerization was simulated using PREDICI with the value of K_{ATRP} measured for this catalyst (~$3x10^{-5}$), the low initiation efficiency observed experimentally was fully consistent with the simulation results (Figure 12S). Thus, despite the presence of 10% Os^{III} deactivator from the onset of the reaction, it seems a large amount of radical termination still occurs due to the exceptional activity of the catalyst. The molecular weight distribution was much more narrow throughout the reaction (M_w/M_n ~ 1.05) than in the analogous system mediated by $RuCl(Cp^*)P^iPr_3$ (M_w/M_n > 1.5). However, high conversion could not be reached (only ~30%) under these conditions with the Os catalyst. It should be noted that a light colored solid precipitated from the polymerization solution after some time, which is reminiscent of the literature observation that derivatives of the arene complex [$OsCp^*(\eta^6\text{-}C_6H_6)$]Br slowly precipitate from aromatic solutions containing $OsBr(Cp^*)P^iPr_3$ over the course of several days at elevated temperatues.[44] The ability of the Os complex to mediate ATRP of acrylates and methacrylates is outside the scope of this manuscript but is currently under investigation.

D. Polymerization Mechanism

1.Organometallic Radical Polymerization (OMRP) Conditions. While Ru is not known to mediate OMRP (Scheme 2) through reversible formation of a Ru^{III}-C bond, in light of the aforementioned trend that transition metal-alkyl bond dissociation energies tend to increase in a group in the order 3d < 4d < 5d,[32] an Os^{III}-C bond is expected to be more stable. It is therefore conceivable that under ATRP conditions, Os^{II} could activate an alkyl halide initiator to generate a radical, and polymerization would actually be mediated through the reversible formation of an

organometallic Os^{III} species. As mentioned, such a situation has been observed and well documented with Mo catalysts. [35-40]

One of the limitations of metal mediated OMRP is that a stoichiometric amount of metal species is required per polymer chain. In contrast, control over molecular weights and molecular weight distributions in ATRP has been achieved with catalyst concentrations more than 100 times lower than is required in OMRP.[15] Thus, how much of the observed control in Os mediated polymerization can be attributed to an OMRP mechanism has direct implications on whether this metal may ever be successfully used at very low catalyst concentrations in ATRP and therefore on whether or not these relatively expensive catalysts may ever find industrial application.

It was recently reported that $OsCl_2(PPh_3)_3$ could successfully mediate a controlled polymerization of styrene under ATRP conditions with an alkyl halide initiator at high temperatures (100 °C),[30] with polydispersity decreasing throughout the reaction from 1.3 to 1.1. The same complex was also reported to mediate growing polystyrene molecular weights under OMRP conditions at the same temperature, whereby AIBN provided a source of radicals in the presence of the $OsCl_2(PPh_3)_3$ compound. Polydispersity in the latter reaction was much higher (M_w/M_n ~3.5) than under ATRP conditions; however, reanalysis of the shape of the GPC traces reveals that the broad molecular weight distribution is due to the presence of many low molecular weight dead chains. As the half-lifetime of AIBN at 100 °C is only ~ 6 min., a very high concentration of radicals would have been quickly generated under these conditions. Figure 7 illustrates the results of an experiment where free radicals are slowly generated by thermal initiation of styrene at 110 °C in (a) the absence of any metal species, (b) the presence of $RuCl_2(PPh_3)_3$, and (c) the presence of $OsCl_2(PPh_3)_3$.

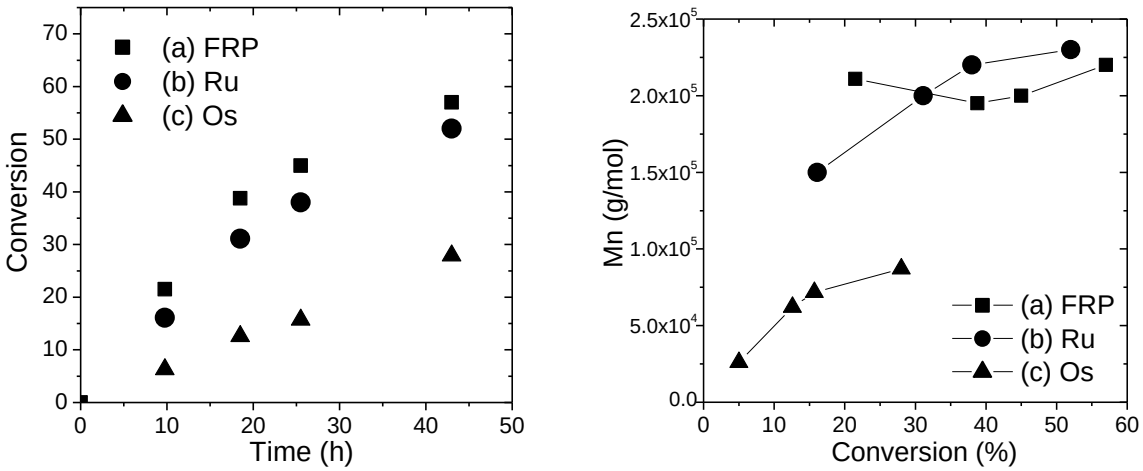

Figure 7. Thermal initiation of styrene, 110°, 50% anisole: (a) no metal (FRP conditions), (b) [Sty]:[$RuCl_2(PPh_3)_3$] = 200:1, and (c) [Sty]:[$OsCl_2(PPh_3)_3$] = 200:1. Mw/Mn for (a) and (b) is > 2.0 in every sample, while for (c) it is initially low (1.3) and then broadens with time.

In the absence of any metal, only high molecular weight polystyrene is generated (M_n ~200K g/mol). In the presence of $RuCl_2(PPh_3)_3$, the results are nearly the same, but the marginally slower polymerization suggests the possibility of a certain degree of radical trapping (*vide infra*). Polydispersity in both systems is > 2.0. With $OsCl_2(PPh_3)_3$, on the other hand, the reaction is about twice slower, and at low conversion (5%), polystyrene molecular weights are about 26K g/mol and M_w/M_n is 1.3 (compared with a M_w/M_n of 1.3 at the beginning of the ATRP reaction mediated with this complex). The molecular weight shows a regular, almost linear increase with conversion, indicating that a certain degree of reversible termination is present. The molecular weight distribution ultimately broadens with time, but this is expected with the slow initiation of new chains.

A similar linear increase in molecular weight with conversion is observed when a free radical initiator is employed to initiate styrene in the presence of $OsBr(Cp^*)P^iPr_3$ at 60 °C (Figure 13S),

although M_w/M_n is again uncontrolled. These experiments alone do not confirm Os can trap radicals via an OMRP mechanism. However, they do suggest that the potential contribution from such a mechanism in Os mediated ATRP warrants further investigation.

2. Polymer chain end analysis. Theoretical calculations (*vide infra*) support the possibility that formation of an Os^{III}-R bond can occur to mediate polymerization under appropriate conditions. Another possible mechanism whereby $OsCl_2(PPh_3)_3$ could mediate growing radical chains involves deactivation of the radicals via reverse ATRP, in which the ATRP equilibrium would be established among Os^I/Os^{II} species, and dormant halide capped chains would be generated. However, when polystyrene of M_n = 10,000 g/mol was generated from AIBN in the presence of $OsCl_2(PPh_3)_3$ ([Sty]:[$OsCl_2(PPh_3)_3$]:[AIBN] = 200:1:2/3, 100 °C, bulk) in 30 min., ^{1}H NMR chain end analysis of the sample (Figure 14S) revealed the absence of any chloride terminated chains, leaving OMRP as the most plausible mechanism to mediate the radical polymerization.

As suggested earlier, it also is conceivable that polymerization initiated under ATRP conditions from Os^{II} and an alkyl halide initiator might be (partially) mediated by OMRP. In an effort to find evidence in favor of this possibility, chain end analysis was again employed. Polystyrene of M_n = 4,200 g/mol was generated in 30 min. under ATRP conditions ([Sty]:[$OsCl_2(PPh_3)_3$]:[PECl] = 200:1:1, 100 °C, bulk). The presence of alkyl chloride end groups (4.45 ppm in $(CD_3)_2CO$) were identified in the ^{1}H NMR analysis of the macroinitiator. Furthermore, after all residual metal species were removed from the sample (see Experimental), the macroinitiator was chain extended with a CuCl catalyst via ATRP. Virtually all of the chains were extended (Figure 8), confirming there had been no significant amount of dormant Os^{III}-R species. The same results were obtained with the OsBr(Cp*)P^{i}Pr$_3$ complex (Figure 15S). Note,

however, that this only represents negative evidence to exclude the intervention of OMRP. Both ATRP and OMRP trapping may occur, but only the Cl-terminated dormant chains may be recovered if the thermodynamic stability of the ATRP dormant species is lower (*vide infra*).

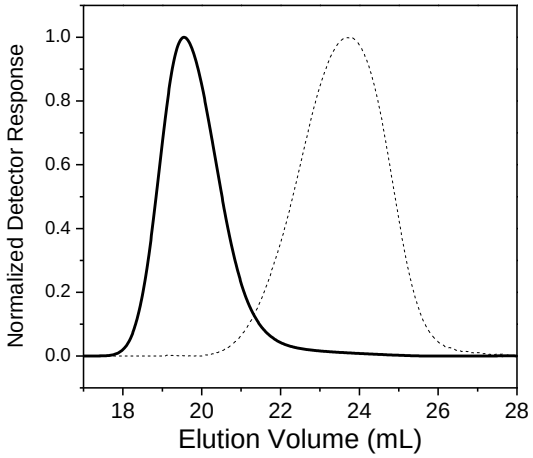

Figure 8: (dashed line) Polystyrene macroinitiator (PSty-Cl) generated under ATRP conditions with $OsCl_2(PPh_3)_3$ ([Sty]:[Os^{II}]:[PECl] = 200:1:1, 100 °C, bulk, 30 min.); (solid line) CuCl(BPMDOA) chain extended polystyrene ([Sty]:[PSty-Cl]:[CuCl]:[$CuCl_2$]:[BPMODA] = 200 : 1 : 1 : 0.1 : 1.1, 100 °C, bulk, ~20 h).

3. Theoretical calculations. In order to evaluate the likelihood that standard halogen atom transfer (for ATRP) and reversible radical trapping (for OMRP) processes are indeed regulating the growing radical concentration, DFT calculations were carried out on models of both $MtCl_2(PPh_3)_3$ (Mt = Ru, Os) systems where the triphenylphosphine ligand was replaced with the computationally less demanding PH_3 ligand. Electronic and steric effects associated to this substitution should not be underestimated,[59-61] but the calculations are believed to at least provide some guidance as to the energy changes involved. Systems $RuCl_2(PH_3)_3$ and *mer*-$RuCl_3(PH_3)_3$ were calculated at the same level of theory and reported previously, as part of another

investigation.[62] A view of the optimized geometries and relative enthalpies for the relevant equilibria are shown in Figure 9 (gas-phase free energies are illustrated in Figure 17S).

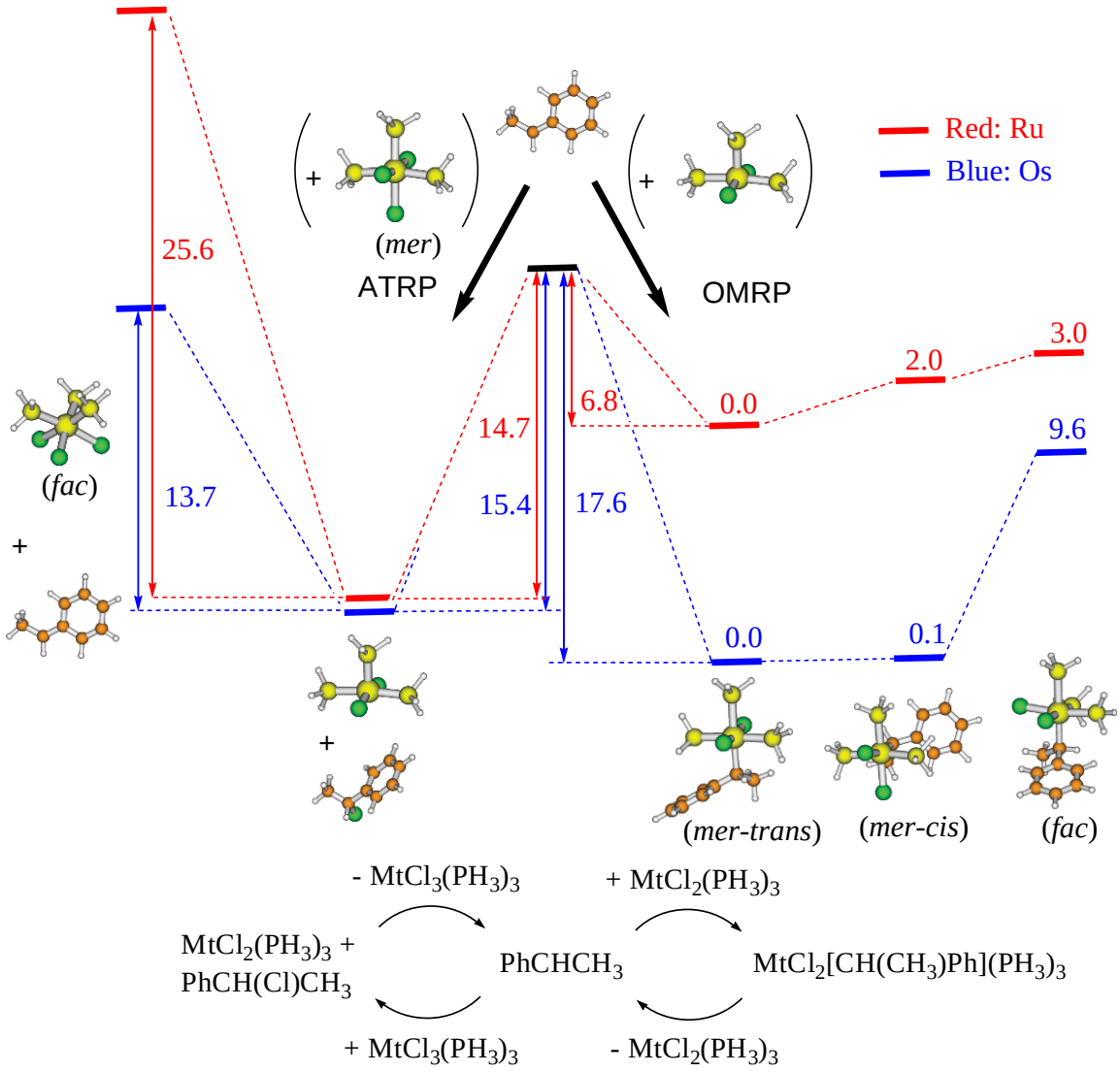

Figure 9. Relative internal energies of Ru and Os complexes used in this theoretical study (*n.b.*, entropy is not considered here). The optimized geometries shown are those of the Os systems.

The optimized geometries are generally in very good agreement with analogous compounds for which the structure was experimentally determined by X-ray diffraction methods. Details are provided in the Supporting Information, which also gives the optimized structures in Cartesian coordinate form (Table 2S) and a table of selected bond distances and angles (Table 3S). For the Ru system, the model ATRP activation reaction leads from the more stable structure of $MtCl_2(PH_3)_3$ to the *mer* isomer of $MtCl_3(PH_3)_3$, which is the energetically more favorable product isomer. For the osmium system, an atom transfer leading to either isomer can be envisaged, because direct atom transfer leads to the higher energy *mer* isomer, whereas an initial rearrangement of the Os^{II} catalyst to a higher-energy geometry having an axial Cl ligand leads to the more stable *fac* product. Stereochemical rearrangements for complexes $MtX_2(PPh_3)_3$ (Mt = Ru, Os; X = Cl, Br) are fast on the NMR timescale.[45] According to the calculations, the ATRP equilibrium is 13.7 kcal mol^{-1} uphill for the generation of the active radical and the oxidized *fac*-$[OsCl_3(PH_3)_3]$ complex. This corresponds to the difference between the bond dissociation energies (BDE) of the $PhCH(CH_3)$-Cl (69.1 kcal mol^{-1}) and Os^{III}-Cl BDE (55.5 kcal mol^{-1}) bonds. The formation of complex *mer*-$[OsCl_3(PH_3)_3]$ requires only a small amount of extra energy (15.4 kcal mol^{-1}). In both cases, the energy difference is in a convenient range for the establishment of a suitable equilibrium with the active radical. In the presence of the sterically more demanding PPh_3 in the real catalyst, and assuming that additional electronic factors affecting the Os-Cl bond strength are unimportant, the energy difference is expected to be somewhat greater. The same process is 14.7 kcal/mol uphill for the Ru system, *i.e.* quite comparable with the calculated values for osmium. Thus, to a first approximation, the calculations agree with the experimental observation that both complexes are ATRP catalysts.

As far as the OMRP equilibrium is concerned, the lowest energy structure for the Mt^{III}-R dormant species corresponds to the mechanistically simpler radical trapping by binding at the vacant site of the $MtCl_2(PH_3)_3$ catalyst. The energy gain associated with the formation of the Mt^{III}-R bond is 17.6 kcal mol^{-1} for Os and only 6.8 kcal mol^{-1} for Ru. As expected, the Mt-R bond is significantly stronger for the heavier atom. For osmium, this energy is slightly greater than the gain associated with the formation of the ATRP dormant species, leading to the prediction that Os-terminated dormant chains could indeed form under ATRP conditions. However, this is opposite to the experimental evidence, because only Cl chain ends are found in the polymer obtained by ATRP as determined by ^1H NMR.

This discrepancy can be reconciled on the basis of two considerations. Firstly, the calculated Os^{III}-R BDE is probably affected by the neglect of the phosphine ligand steric bulk to a greater extent than the Os^{III}-Cl BDE. Thus, the OMRP dormant species would in reality be less favored, relative to the ATRP dormant species. Secondly, and perhaps most importantly, the OMRP equilibrium is much more affected by the entropic part of the free energy than the ATRP equilibrium. In fact, the former implicates the disappearance of one molecule with consequent elimination of three translational degrees of freedom, whereas the latter implicates the same number of molecules on each side of the equilibrium. An estimation of the free energy change in solution is not easily accessible, since the entropy available from the DFT calculations refers to the gas phase. Upon going from the gas phase to the solution phase, the entropy is partially but not totally quenched, since the free translations and rotations (especially the former) are transformed into more constrained and complex tumbling modes upon the influence of the neighboring solvent molecules. A simple method to quantify this entropy reduction is not currently available. We report in Table 3 a comparison of calculated energies, enthalpies, and

free energies (gas phase). As can be seen from the table, the values corresponding to the ATRP equilibrium are relatively unaffected since the translational entropy of both sides of the equilibrium is essentially identical. The values corresponding to the OMRP equilibrium, on the other hand, are highly affected by the entropic component. Keeping the above qualitative arguments in mind we can conclude that, for Os, the simultaneous reversible formation of ATRP and OMRP dormant species, though the first one is more stable and is ultimately found in the isolated polymer, contributes to further lower the free radical concentration under polymerization conditions, improving the catalyst controlling ability. However, the energetic balance is considerably less favorable to OMRP trapping for the Ru system.

Table 3. Computed changes, in kcal mol^{-1}, related to the ATRP and OMRP equilibria

	ΔE	ΔH_{298}	ΔG_{298} (gas phase)	~~ΔG_{298} (no trans. S)~~
[a]$R + RuCl_3 \rightarrow R\text{-}Cl + RuCl_2$	-14.65	-12.94	-12.45	~~-12.30~~
$R + OsCl_3 \rightarrow R\text{-}Cl + OsCl_2$	-13.66	-12.27	-13.24	~~-13.07~~
$R + RuCl_2 \rightarrow RuCl_2R$	-6.83	-4.95	8.84	~~-2.75~~
$R + OsCl_2 \rightarrow OsCl_2R$	-17.58	-15.29	0.92	~~-10.73~~

[a]*mer* isomer for Ru; *fac* isomer for Os.

Conclusions

Several important discoveries and contributions were made to the field in this work.

1. Ru and Os ATRP catalysts of the formula $MtX(Cp^*)P^iPr_3$ are on the order of a half a volt less reducing than Cu catalysts of comparable activity. Evaluation of kinetic polymerization data, together with $E_{1/2}$ and K_{ATRP} values, suggests that halide affinities of these Ru and Os compounds must be approximately 7-9 orders of magnitude stronger than typical Cu ATRP catalysts to compensate for their comparatively poor reducing power. This method not only provides a way to screen ATRP catalysts based on the stability of their Mt-X bond; it may also provide an

indirect way to determine values of K_X that are otherwise too high to quantify with spectroscopic measurements.

2. OsBr(Cp*)P^{i}Pr$_3$ proved one of the most active ATRP complexes known to date (K_{ATRP} with PEBr in tetrahydrofuran = 3.2×10^{-5}), being over 10,000 times more active than its RuCl(Cp*)P^{i}Pr$_3$ analogue with PECl. Being so active makes the Os catalyst an excellent candidate for use at low catalyst concentrations.

3. The ability of the coordinatively unsaturated Os compounds to control polystyrene molecular weights under OMRP conditions where the Ru analogues and Cu compounds could not was rationalized in terms of the intrinsic ability of Os to form strong Mt-C bonds and was supported with theoretical calculations. Despite the ability of the Os compounds to mediate growing polystyrene molecular weights under OMRP conditions, they predominantly catalyze ATRP in the presence of an alkyl halide initiator.

With such strong halidophilicities and the ability to mediate ATRP, these active Ru and Os catalysts remain promising candidates for challenging systems that require low catalyst concentrations under conditions where Cu-X bonds are susceptible to hydrolysis or dissociation.

Acknowledgement. The authors thank the members of the ATRP/CRP consortia at Carnegie Mellon University and NSF (grants CHE-0405627 and DMR-0549353) for funding. WAB thanks the Harrison Legacy Dissertation Fellowship for financial support. RP thanks CINES and CICT (project CALMIP) for a grant of free computer time.

Supporting Information Available: electronic spectra of all relevant compounds; plots used in the determination of all K_{ATRP} values; M_n and M_w/M_n vs. conversion data for polymerizations; ^{1}H NMR spectra; chain extension data; PREDICI simulations; Cartesian

coordinates for all DFT-optimized geometries; selected bond distances and angles optimized by DFT calculations; and complete ref 50. This material is available free of charge via the Internet at http://pubs.acs.org.

References

(1) Wang, J.-S.; Matyjaszewski, K. *J. Am. Chem. Soc.* **1995**, *117*, 5614-5615.

(2) Kato, M.; Kamigaito, M.; Sawamoto, M.; Higashimura, T. *Macromolecules* **1995**, *28*, 1721-1723.

(3) Coessens, V.; Pintauer, T.; Matyjaszewski, K. *Prog. Polym. Sci.* **2001**, *26*, 337-377.

(4) Pyun, J.; Matyjaszewski, K. *Chem. Mater.* **2001**, *13*, 3436-3448.

(5) Davis, K. A.; Matyjaszewski, K. *Adv. Polym. Sci.* **2002**, *159*, 1-166.

(6) Matyjaszewski, K. *Macromol. Symp.* **2003**, *195*, 25-31.

(7) Matyjaszewski, K.; Xia, J. *Chem. Rev.* **2001**, *101*, 2921-2990.

(8) Kamigaito, M.; Ando, T.; Sawamoto, M. *Chem. Rev.* **2001**, *101*, 3689-3745.

(9) Braunecker, W. A.; Matyjaszewski, K. *Prog. Polym. Sci.* **2007**, *32*, 93-146.

(10) Tsarevsky, N. V.; Pintauer, T.; Matyjaszewski, K. *Macromolecules* **2004**, *37*, 9768-9778.

(11) Tsarevsky, N. V.; Braunecker, W. A.; Brooks, S. J.; Matyaszewski, K. *Macromolecules* **2006**, *39*, 6817-6824.

(12) Wakioka, M.; Baek, K.-Y.; Ando, T.; Kamigaito, M.; Sawamoto, M. *Macromolecules* **2002**, *35*, 330-333.

(13) Tang, H.; Arulsamy, N.; Sun, J.; Radosz, M.; Shen, Y.; Tsarevsky, N. V.; Braunecker, W. A.; Tang, W.; Matyjaszewski, K. *J. Am. Chem. Soc.* **2006**, *128*, 16277-16285.

(14) Jakubowski, W.; Matyjaszewski, K. *Angew. Chem., Int. Ed.* **2006**, *45*, 4482-4486.

(15) Matyjaszewski, K.; Min, K.; Tang, W.; Huang, J.; Braunecker, W. A.; Tsarevsky, N. V.; Jakubowski, W. *Proc. Natl. Acad. Sci. (U.S.A.)* **2006**, *103*, 15309-15314.

(16) Tang, W.; Tsarevsky, N. V.; Matyjaszewski, K. *J. Am. Chem. Soc.* **2006**, *128*, 1598-1604.

(17) Tang, W.; Kwak, Y.; Tsarevsky, N. V.; Matyjaszewski, K. *Polym. Prep. (Am. Chem. Soc., Div. Polym.Chem.)* **2007**, *48*, 392-393.

(18) Gillies, M. B.; Matyjaszewski, K.; Norrby, P.-O.; Pintauer, T.; Poli, R.; Richard, P. *Macromolecules* **2003**, *36*, 8551-8559.

(19) Pintauer, T.; McKenzie, B.; Matyjaszewski, K. *ACS Symp. Ser.* **2003**, *854*, 130-147.

(20) Qiu, J.; Matyjaszewski, K.; Thouin, L.; Amatore, C. *Macromol. Chem. Phys.* **2000**, *201*, 1625-1631.

(21) Matyjaszewski, K.; Goebelt, B.; Paik, H.-j.; Horwitz, C. P. *Macromolecules* **2001**, *34*, 430-440.

(22) Tsarevsky, N. V.; Braunecker, W. A.; Tang, W.; Brooks, S. J.; Matyjaszewski, K.; Weisman, G. R.; Wong, E. H. *J. Mol. Catal. A: Chem.* **2006**, *257*, 132.

(23) O'Reilly, R. K.; Gibson, V. C.; White, A. J. P.; Williams, D. J. *J. Am. Chem. Soc.* **2003**, *125*, 8450-8451.

(24) O'Reilly, R. K.; Gibson, V. C.; White, A. J. P.; Williams, D. J. *Polyhedron* **2004**, *23*, 2921-2928.

(25) Ando, T.; Kamigaito, M.; Sawamoto, M. *Macromolecules* **2000**, *33*, 5825-5829.

(26) Richel, A.; Demonceau, A.; Noels, A. F. *Tetrahedron Lett.* **2006**, *47*, 2077-2081.

(27) Delaude, L.; Demonceau, A.; Noels, A. F. *Top. Organomet. Chem.* **2004**, *11*, 155-171.

(28) Brumaghim, J. L.; Girolami, G. S. *Organometallics* **1999**, *18*, 1923-1929.

(29) Cobo, N.; Esteruelas, M. A.; Gonzalez, F.; Herrero, J.; Lopez, A. M.; Lucio, P.; Olivan, M. *J. Catalysis* **2004**, *223*, 319-327.

(30) Braunecker, W. A.; Itami, Y.; Matyjaszewski, K. *Macromolecules* **2005**, *38*, 9402-9404.

(31) Lever, A. B. P. *Inorg. Chem.* **1990**, *29*, 1271-1285.

(32) Mancuso, C.; Halpern, J. *J. Organomet. Chem.* **1992**, *428*, C8-C11.

(33) footnote1.

(34) Wayland, B. B.; Poszmik, G.; Mukerjee, S. L.; Fryd, M. *J. Am. Chem. Soc.* **1994**, *116*, 7943-7944.

(35) Le Grognec, E.; Claverie, J.; Poli, R. *J. Am. Chem. Soc.* **2001**, *123*, 9513-9524.

(36) Stoffelbach, F.; Poli, R.; Richard, P. *J. Organomet. Chem.* **2002**, *663*, 269-276.

(37) Stoffelbach, F.; Haddleton, D. M.; Poli, R. *Eur. Polym. J.* **2003**, *39*, 2099-2105.

(38) Maria, S.; Stoffelbach, F.; Mata, J.; Daran, J.-C.; Richard, P.; Poli, R. *J. Am. Chem. Soc.* **2005**, *127*, 5946-5956.

(39) Poli, R.; Stoffelbach, F.; Maria, S. *Polym. Prep. (Am. Chem. Soc., Div. Polym.Chem.)* **2005**, *46*, 305-306.

(40) Poli, R. *Angew. Chem., Int. Ed.* **2006**.

(41) Shaver, M. P.; Allan, L. E. N.; Rzepa, H. S.; Gibson, V. C. *Angew. Chem., Int. Ed.* **2006**, *45*, 1241-1244.

(42) Campion, B. K.; Heyn, R. H.; Tilley, T. D. *J. Chem. Soc., Chem. Comm.* **1988**, 278-280.

(43) Arliguie, T.; Chaudret, B. *J. Chem. Soc., Chem. Comm.* **1986**, 985-986.

(44) Glaser, P. B.; Tilley, T. D. *Eur. J. Inorg. Chem.* **2001**, 2747-2750.

(45) Hoffman, P. R.; Caulton, K. G. *J. Am. Chem. Soc.* **1975**, *97*, 4221-4228.

(46) Khan, M. M. T.; Ahamed, S. S.; Levenson, R. A. *J. Inorg. Nucl. Chem.* **1976**, *38*, 1135-1138.

(47) Xia, J.; Matyjaszewski, K. *Macromolecules* **1999**, *32*, 2434-2437.

(48) Wulkow, M. *Macromol. Theor. Simul.* **1996**, *5*, 393-416.

(49) Becke, A. D. *J. Chem. Phys.* **1993**, *98*, 5648-5652.

(50) Frisch, M. J.; et al. *Gaussian 03, Revision B.04*; Gaussian, Inc.: Pittsburgh PA, 2003.

(51) Hay, P. J.; Wadt, W. R. *J. Chem. Phys.* **1985**, *82*, 270-283.

(52) Takeuchi, K. J.; Thompson, M. S.; Pipes, D. W.; Meyer, T. J. *Inorg. Chem.* **1984**, *23*, 1845-1851.

(53) Baitalik, S.; Florke, U.; Nag, K. *Inorg. Chim. Acta* **2002**, *337*, 439-449.

(54) Shipp, D. A.; Matyjaszewski, K. *Macromolecules* **1999**, *32*, 2948-2955.

(55) Shipp, D. A.; Matyjaszewski, K. *Macromolecules* **2000**, *33*, 1553-1559.

(56) Tang, W.; Fukuda, T.; Matyjaszewski, K. *Macromolecules* **2006**, *39*, 4332-4337.

(57) Poon, C.-K.; Isabirye, D. A. *J. Chem. Soc., Dalton Trans.* **1977**, 2115-2120.

(58) Watanabe, Y.; Ando, T.; Kamigaito, M.; Sawamoto, M. *Macromolecules* **2001**, *34*, 4370-4374.

(59) Schmid, R.; Herrmann, W. A.; Frenking, G. *Organometallics* **1997**, *16*, 701-708.

(60) Gonzáles-Blanco, O.; Branchadell, V. *Organometallics* **1997**, *16*, 5556-5562.

(61) Haeberlen, O. D.; Roesch, N. *J. Phys. Chem.* **1993**, *97*, 4970-4973.

(62) Poli, R.; Stoffelbach, F.; Maria, S.; Mata, J. *Chem. Eur. J.* **2005**, *11*, 2537-2548.

Table of Contents Graphic